Chapter 17

Cellular Application of Genetically Encoded Sensors and Impeders of AMPK

Takafumi Miyamoto, Elmer Rho, Allen Kim, and Takanari Inoue

Abstract

Unraveling the spatiotemporal dynamics of 5'-AMP-activated protein kinase (AMPK) signaling is necessary to bridge the gap between nutrient signaling and downstream function. Three genetically encoded Förster Resonance Energy Transfer (FRET)-based AMPK biosensors are available yielding insight into how AMPK-derived signal propagates throughout a cell in response to particular inputs. These findings, together with accumulating evidence obtained from biochemical techniques, promise to give a holistic understanding of the AMPK signaling. In this protocol, we describe the procedures and materials required for imaging intracellular AMPK activity in an organelle-specific manner, with a focus on ABKAR, a FRET-based biosensor. In addition, we introduce a novel AMPK inhibitor peptide that allows us to inhibit AMPK activity at specific subcellular compartments.

Key words Organelle-specific, Kinase activity monitoring, Biosensor, Förster resonance energy transfer (FRET), Compartmentalization, Signaling dynamics, Inhibitor peptide

1 Introduction

The mammalian 5'-AMP-activated protein kinase (AMPK) is a heterotrimeric enzyme composed of a catalytic α subunit, scaffold β subunit, and regulatory γ subunits [1]. There are two genes encoding isoforms of both the α and β subunits (α1 and α2, β1 and β2) and three genes encoding isoforms of the γ subunit (γ1, γ2, and γ3) [2]. AMPK senses changes in intracellular energy by responding to the relative levels of ATP compared to either AMP or ADP. For AMPK to be fully activated, AMP and/or ADP binds to the γ subunit of AMPK. This leads to a conformational change of AMPK [3, 4] that exposes amino acid Thr172 within the activation loop of the α subunit, allowing it to be subsequently phosphorylated and activated by the upstream AMPK kinases such as LKB1 [5] and CaMKKβ [6, 7].

Once activated, AMPK phosphorylates downstream substrates to regulate critical cellular functions such as metabolic homeostasis,

Dietbert Neumann and Benoit Viollet (eds.), *AMPK: Methods and Protocols*, Methods in Molecular Biology, vol. 1732, https://doi.org/10.1007/978-1-4939-7598-3_17,

cell growth, proliferation, autophagy, polarity, and transcription. So far, over 50 proteins have been identified as AMPK substrates [8]. Notably, these substrates are present in various subcellular compartments (Table 1), suggesting a role for spatial regulation of AMPK activity.

The signaling dynamics of AMPK have been studied extensively with biochemical assays [1, 2]. However, the experimental methods used to assess the signaling dynamics of AMPK are limited because of the daunting task of visualizing these processes at the subcellular compartment level in living cells in real time. Therefore, the spatio-temporal dynamics of AMPK signaling have remained mostly unknown until the recent advent of imaging techniques based on Förster Resonance Energy Transfer (FRET).

FRET is a physical process by which energy transfers from an excited donor fluorophore to an acceptor fluorophore through non-radiative dipole-dipole coupling [9]. Since the efficiency of the energy transfer depends on the donor-acceptor distance and/or their relative orientation, FRET has been widely used to monitor protein-protein interactions and protein conformational changes. Among many applications, genetically encoded FRET-based biosensors have been exploited to visualize various kinase dynamics in living cells. These kinase activity reporters (KARs) consist of a pair of fluorophores that have sufficient spectral overlap, an optimized substrate motif of the target kinases, and a phosphopeptide-binding forkhead-associated (FHA1) domain. Phosphorylation of the substrate motif increases its affinity toward FHA1 domain, bringing donor and acceptor fluorophores such that FRET. Based on these principles, three FRET-based AMPK biosensors have been developed: AMPKAR, ABKAR, and BimAB-KAR (Fig. 1).

The first generation of the biosensor called AMPKAR is a unimolecular FRET biosensor [10]. The structural layout is similar to many other KARs. It consists of ECFP and circularly permuted variants of Venus cpV E172 as a fluorophore FRET pair, bracketing an FHA1 domain and an AMPK substrate motif. When AMPK is activated, AMPKAR undergoes conformational changes that lead to an increase of the FRET signal. The use of AMPKAR thus allows for visualization of AMPK dynamics in either cytoplasmic or nuclear compartment under different experimental conditions; however, there still exists a need to monitor AMPK activity with subcellular resolution to capture spatially differentiated dynamics. ABKAR, a second-generation AMPK biosensor, lived up to this demand [11–13]. It was achieved by having the donor fluorophore, ECFP, in AMPKAR replaced with Cerulean 3, a brighter version of ECFP, resulting in an approximately two-fold larger dynamic range relative to the original AMPKAR. Additional refinements were

Table 1
A list of AMPK substrates and their main localization

Protein name	Gene name	Main localization
Girdin	CCDC88A	Cell-cell junction
Acetyl-CoA carboxylase 1	ACACA	Cytosol
Insulin receptor substrate 1	IRS1	Cytosol
TBC1 domain family member 4	TBC1D4	Cytosol
Troponin I, cardiac muscle	TNNI3	Cytosol
Tuberous sclerosis complex 2	TSC2	Cytosol
Serine/threonine-protein kinase ULK1	ULK1	Cytosol
Lactate dehydrogenase	LDH	Cytosol
3-Hydroxy-3-methylglutaryl-coenzyme A reductase	HMGCR	ER
Golgi-specific brefeldin A-resistance guanine nucleotide exchange factor 1	GBF1	Golgi apparatus
Sterol regulatory element-binding protein 1	SREBP-1c	Golgi apparatus
Regulatory-associated protein of mTOR	RPTOR	Lysosome
Protein kinase C theta	PRKCQ	Microtubule organizing center
CAP-Gly domain-containing linker protein 1	CLIP-170	Microtubules
Glycogen synthase 1 (muscle isoform)	GYS1	Microtubules, cytosol
Acetyl-CoA carboxylase 2	ACACB	Mitochondria
Mitochondrial fusion factor	MFF	Mitochondria
Histone deacetylase 5	HDAC5	Nuclear speckles
1-Phosphatidylinositol 3-phosphate 5-kinase	PIKFYVE	Nuclear speckles
Glutamine-fructose-6-phosphate aminotransferase [isomerizing] 1	GFPT1	Nucleoli
RNA polymerase I-specific transcription initiation factor RRN3	RRN3	Nucleoli
TBC1 domain family member 1	TBC1D1	Nucleoli
Cell division cycle protein 27 homolog	CDC27	Nucleoplasm
CREB-regulated transcription coactivator 2	CRTC2	Nucleoplasm
Eukaryotic elongation factor 2 kinase	eEF2K	Nucleoplasm
Histone acetyltransferase p300	EP300	Nucleoplasm
Histone H2B	H2B	Nucleoplasm
p53	p53	Nucleoplasm

(continued)

Table 1
(continued)

Protein name	Gene name	Main localization
Peroxisome-proliferator-activated receptor gamma coactivator 1-alpha	PGC1A	Nucleoplasm
Tumor protein p73	TP73	Nucleoplasm
Cyclin-dependent kinase inhibitor 1B	CDKN1B	Nucleus
Forkhead box protein O3	FOXO3a	Nucleus
Mdm4	MDM4	Nucleus
6-Phosphofructo-2-kinase/fructose-2,6-bisphosphatase 2	PFKFB2	Nucleus
Hepatocyte nuclear factor 4	HNF4	Nucleus
Carbohydrate-responsive element-binding protein	MLXIPL	Nucleus
Phosphatase 1 regulatory subunit 12C	PPP1R12C	Nucleus
Serine/threonine-protein kinase PAK 2		
Astrocytic phosphoprotein PEA-15	PEA15	Nucleus, cytosol
Clock component cryptochrome 1	CRY1	Nucleus, nuclear membrane, microtubules
Serine/threonine-protein kinase PAK 2	PAK2	Nucleus, vesicles
Microtubule-associated protein tau	MAPT	Plasma membrane
Phospholipase D1	PLD1	Plasma membrane
Thioredoxin-interacting protein	TXNIP	Plasma membrane
Vasodilator-stimulated phosphoprotein	VASP	Plasma membrane, cell junctions, focal adhesion sites
Brain-specific angiogenesis inhibitor 1-associated protein 2	BAIAP2	Plasma membrane, cytosol
Cingulin	CGN	Tight junctions
Serine/threonine-protein kinase B-raf	BRAF	Vesicle

made by fusing a series of organelle-targeting sequences (OTS) to ABKAR (osABKARs) targeting it to various subcellular localizations. A collection of osABKARs allowed for monitoring the AMPK dynamics at various subcellular compartments such as the plasma membrane, Golgi apparatus, endoplasmic reticulum (ER), mitochondria, and lysosomes as well as previously reported cytosolic and nuclear compartments (Fig. 2).

In addition to these unimolecular AMPK biosensors, bimolecular kinase activity reporter for AMPK (BimABKAR) was also developed [14]. In this system, the donor fluorophore

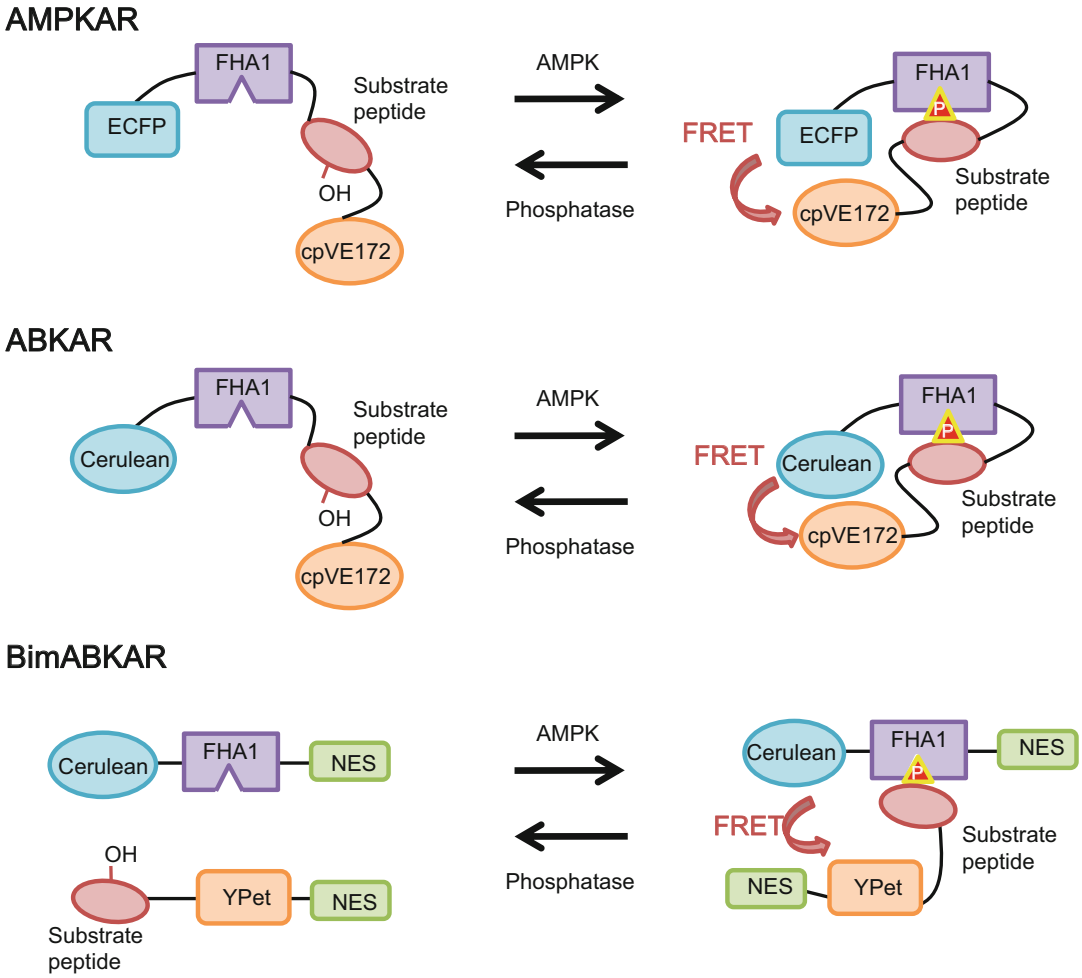

Fig. 1 Schematic diagram of FRET-based AMPK biosensors. *ECFP* enhanced cyan fluorescent protein, *cpVE172* circularly permuted variants of Venus cpV E172, *FHA1* forkhead-associated domain1, *Cerulean* cerulean 3, *YPet* yellow fluorescent protein (YFP) variant, *NES* nuclear export signal. Reproduced from [11] with permission

(Cerulean)-fused FHA1 domain and the acceptor fluorophore (YPet)-fused AMPK substrate motif were expressed as two different proteins. By appending an OTS (e.g., KRAS for plasma membrane) to a YPet-fused AMPK substrate motif, the BimABKARs, like the osABKARs, were also able to reveal activation dynamics of AMPK at specific subcellular compartments. To that end, subcellular compartment-specific BimABKAR succeeded in illuminating the cross talk of AMPK and cAMP-dependent protein kinase signaling at the plasma membrane [14]. Collectively, these reporters have revealed a role for compartmentalized AMPK signaling.

One of the downsides of currently available approaches in manipulating AMPK activity is their spatial non-specificity. For

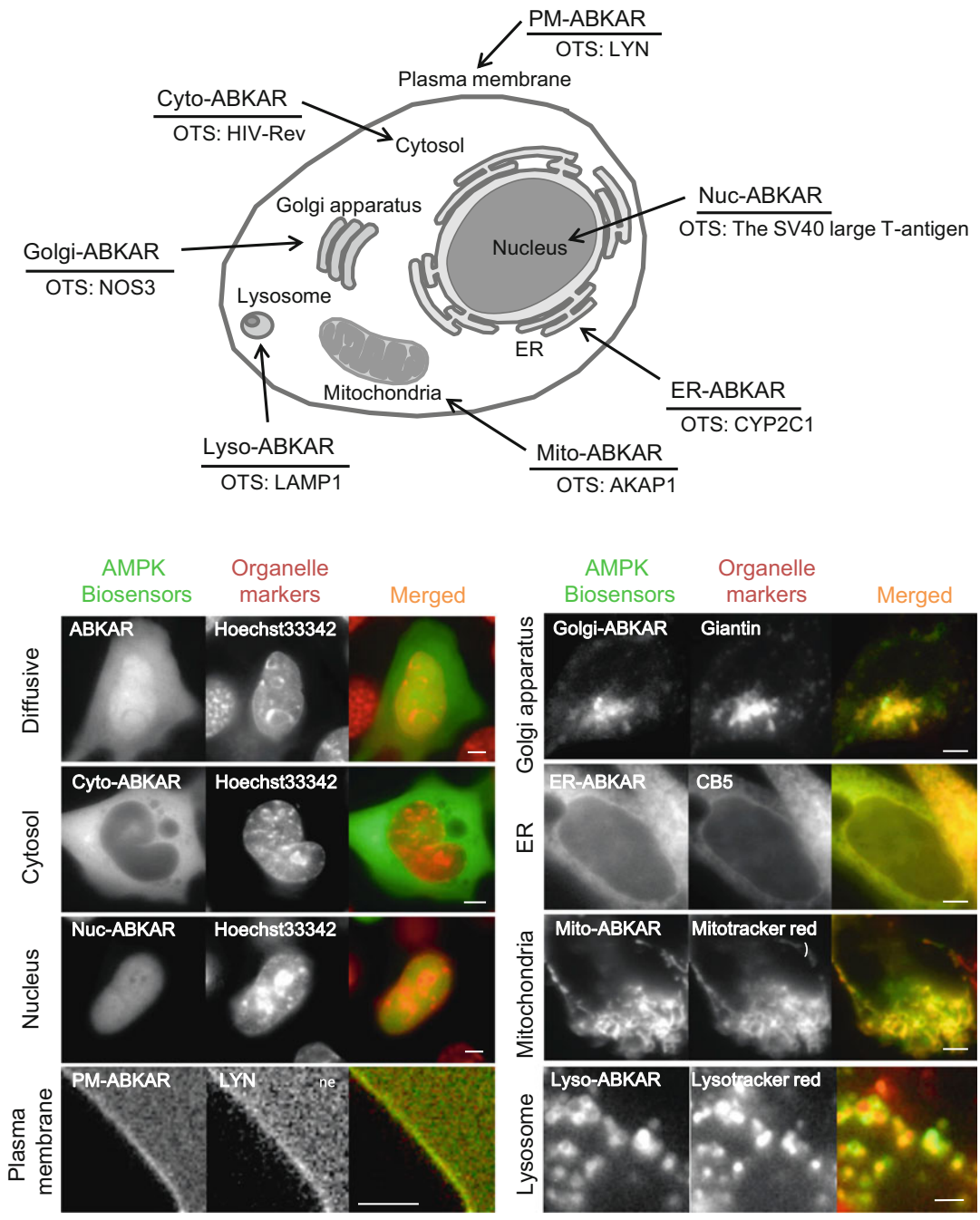

Fig. 2 The localization of organelle-specific ABKARs. Scale bar, 10 μm. Reproduced from [11] with permission

example, 2-deoxyglucose and ionomycin have been used to globally activate AMPK through activation of LKB1 and CaMKKβ, respectively, and Compound C is used for global inhibition of AMPK. Due to the global nature of these perturbations, these

approaches are unsuitable for studying compartmentalized signaling. Development of a tool to precisely target AMPK activity will further enrich our understanding of AMPK signaling. Recently, an AMPK inhibitor peptide (AIP) has been developed which now allows us to inhibit AMPK activity at specific subcellular compartments.

To date, two types of AIPs are available: AIP and the phosphorylation site-mutated version, AIP (TA) (Fig. 5a). Each version is suited for different purposes, and the choice between the two AIPs should be based on the careful discretion of the experimenter. AIP is applicable to experiments where chronic inhibition of AMPK at a subcellular compartment is demanded. In contrast, AIP (TA) is less effective but allows the experimenter to have control of the onset of inhibition at specific compartments with the help of dimerization methods such as chemically induced dimerization (CID) [11, 15].

Although the application of these FRET-based AMPK biosensors has yielded important insights into the AMPK signaling network throughout the cell, our understanding of compartmentalized AMPK signaling is far from complete. In the protocol below, we describe some general principles and optimization schemes to measure the spatiotemporal dynamics of AMPK activity in living cells using ABKAR/osABKARs. Briefly, the experimenter will measure compartmentalized AMPK signaling dynamics via four simple steps: (1) preparation of plasmid DNA encoding ABKAR/osABKARs and AIP, (2) conventional transfection of the plasmid DNA into target cells, (3) imaging the transfected cells using fluorescent microscopy, and (4) data analysis using image analysis software. Details are described below.

2 Materials

2.1 Cell Culture and Transfection

1. CO_2 incubator for cell culture.
2. 6-Well cell culture plate.
3. Opti-MEM reduced serum medium.
4. 0.05% Trypsin-EDTA (*see* **Note 1**).
5. Phosphate-buffered saline (PBS), pH 7.4.
6. Plasmids: 1 mg/ml plasmid DNA encoding ABKAR, osABKARs, and AIP in sterile water. Plasmids encoding osABKARs are available from Addgene.
7. Transfection reagents: In the described experiments, we used FuGENE HD, but other transfection reagents can also be used (*see* **Note 2**).
8. Sterilize round glass cover slips (0.1–0.2 mm thickness and 25 mm diameter).
9. Absolute ethanol.

10. Poly-D-lysine solution (0.1 mg/ml).
11. Milli-Q water.
12. Coverslip holder: serves as a chamber to hold cover slips for cell imaging (for details, *see* [16]).

2.2 Fluorescence Microscopy Imaging and Analysis

1. Physiological stimulant (such as 2-deoxyglucose (2-DG)): 1000× stock solution should be prepared according to manufacturer's instructions (*see* **Note 3**).
2. Imaging medium: phenol red-free DMEM with 25 mM HEPES, pH 7.4 under 5–10% CO_2 environment (*see* **Notes 4–6**).
3. Fluorescence microscopy: In our laboratory, live cell measurements are performed using an epifluorescence microscope. CFP and YFP excitation are carried out by an X-Cite Series 120Q mercury-vapor lamp and processed through appropriate filter cubes. Images are taken using a 63× objective (Plan-Apochromat, NA = 1.4) mounted on an inverted Axiovert 135 TV microscope and are captured by a QIClick charge-coupled device camera. The microscope is operated by the MetaMorph software package. CFP and YFP channels are configured to use the respective excitation and emission filter (427/10 nm excitation and 472/30 nm emission for CFP, 504/12 nm excitation and 542/27 nm emission for YFP), while the FRET channel is configured to use CFP as excitation and YFP as emission.
4. Image analysis software (e.g., MetaMorph imaging software) (*see* **Note 7**).

3 Methods

3.1 osABKAR Design and Preparation

1. Selecting the appropriate OTS is critical for proper osABKAR function. OTSs that were used in previously developed osABKARs are summarized in Fig. 2 (*see* **Note 8**). For targeting to relatively small subcellular compartments (e.g., centrosome, basal body of primary cilia, etc.), it is essential to identify the shortest sequence that effectively targets the sensor to the appropriate compartment. Furthermore, the compartment-specific targeting sequence needs to be as short as possible without degrading the FRET efficiency of ABKAR and is tagged to either the N-terminal or the C-terminal end of ABKAR (*see* **Note 9**). The information on protein localization sequences can be easily obtained online as it is now universally available (e.g., The Human Protein Atlas, http://www.proteinatlas.org/).
2. Prepare the plasmids according to standard subcloning protocols (*see* **Note 10**). Validate all plasmids by sequencing.

3.2 Cell Preparation and Transfection

1. Cultured cells: Maintain cultured cells (e.g., mouse embryonic fibroblasts, HeLa cervical cancer cells, Cos7 African green monkey fibroblasts, etc.), at 37 °C in 5% CO_2 at 90% relative humidity in the appropriate cell culture medium (*see* **Note 11**).
2. Pre-warm cell culture media, Opti-MEM, and trypsin at 37 °C.
3. Prepare the transfection mixture in a 1.5 ml sterile microcentrifuge tube. For FuGENE HD transfection, mix 2 μg of plasmid DNA encoding the desired osABKAR and 6 μl of FuGENE HD in 100 μl Opti-MEM. If multiple constructs are transfected together, the ratio should be optimized by testing the expression of each construct. Transfection reagents are not limited to FuGENE HD, and other transfection reagents (e.g., Lipofectamine) can be used instead. If resorting to a different transfection reagent, the protocol must be modified according to the manufacturer's instruction.
4. Incubate the transfection mixture for 20 min at room temperature (*see* **Note 12**).
5. In the meantime, prepare glass cover slips coated with poly-D-lysine. Store cover slips in individual wells in a 6-well plate (*see* **Note 13**).
6. Trypsinize cells, transfer 210×10^4 number of cells into a 15 ml tube, and spin them down at $362 \times g$ for 3 min (*see* **Note 14**).
7. Resuspend the cells in 10 ml of cell culture medium.
8. Add 500 μl of resuspended cells to 100 μl of the transfection mixture, and mix them well by tapping.
9. Add 80 μl of the cell suspension onto each cover slip.
10. For cell adhesion, leave the cover slips in the incubator for 2 h. Duration of the incubation should be adjusted for individual cell types.
11. Add 2 ml of fresh cell culture medium to each well.
12. Acquire images 36–48 h after transfection (*see* **Note 15**).

3.3 Live Cell Imaging

Monitoring AMPK activity with ABKAR/osABKARs is performed as follows:

1. Replace culture medium with fresh culture medium 2 h before live cell imaging (*see* **Note 16**).
2. Place a cover slip into a metal frame filled with 450 μl of the imaging medium (*see* **Note 17**).
3. Use a fluorescence microscope for image acquisition. Consistent temperature and CO_2 conditions are desirable irrespective of the duration of the imaging session (*see* **Notes 18** and **19**).

4. Under the microscope, select cells for monitoring in the live imaging mode. These cells should contain all the constructs required for the monitoring, which should be confirmed by checking appropriate fluorescence signals. Cells that are unusually dim or bright or that show aberrant organelle morphology should not be selected (*see* **Note 20**).
5. Start the YFP, CFP, and FRET image acquisition in a time-lapse mode. The time frame should be determined depending on the event to be monitored. Usually, observable changes in AMPK activity detected by ABKAR occur within a few minutes after the activation of CaMKKβ-mediated pathway by ionomycin, whereas over 5 min is required for the LKB1-mediated pathway to be activated by perturbing the glycolysis pathways (*see* **Note 21**).
6. Start the imaging without the stimulant to measure the baseline activity of AMPK, and at the desired time point, add the physiological stimulant (*see* **Note 22**).
7. Acquire images until the event of interest is complete. The duration of the imaging session will depend on the expected time range in which you expect to see changes in AMPK activity.

3.4 Data Analysis

The obtained fluorescent images are analyzed as follows:

1. Evaluate AMPK activity by taking regions of interest (ROI) (*see* **Note 23**). Images acquired in a microscope also include contributions from non-FRET fluorescence. The FRET component of the signal can be isolated by calculating the corrected *FRET (FRETc)* (*see* **Note 24**) (Fig. 3).
2. AMPK activity can be calculated from the following equation:

$$\text{AMPK activity} = \frac{\text{FRETc}}{\text{CFP}}$$

3. Once the images are correctly processed, kinase activity will be reflected by the intensity of the pixel in the FRET image. Typically, imaging applications allow various methods of visualizing these intensities. The recommended approach is to visualize the FRET image using a pseudocolor lookup table (LUT). This will create an image where different colors map to different intensity levels (Fig. 4) (*see* **Note 25**).

3.5 Examples of Applications

A genetically encoded AMPK inhibitor peptide (AIP) is a powerful tool to inhibit AMPK activity at specific subcellular compartments (Fig. 5a) (*see* **Note 26**) [11]. The specificity of AIP to AMPK is determined by the amino acid sequence. Thus, the AIP should be rationally designed by utilizing the rich resources that are available

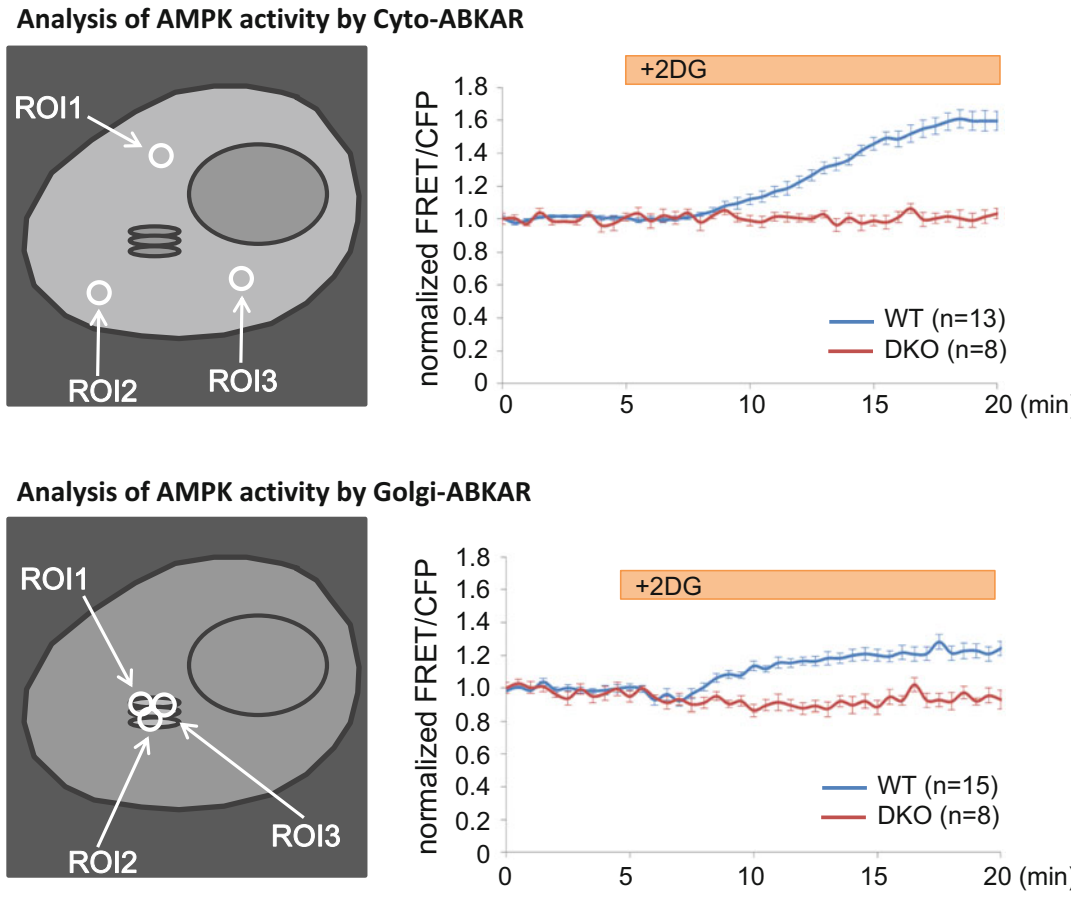

Fig. 3 Examination of AMPK activity by ABKAR. Wild-type MEFs and AMPK α subunit double knockout (DKO) MEFs were treated with 10 mM 2-DG. AMPK activity was measured by indicated AMPK biosensors. Reproduced from [11] with permission

elsewhere [8]. Current versions of the AIP could suppress 10 mM 2-DG-induced AMPK activation in Cos7 cells as measured by ABKAR (Fig. 5b) (*see* **Note 27**) [11]. To develop subcellular compartment-specific AIPs, tag appropriate OTS to the AIP. The inhibitory effect of OTS-fused AIPs can be assessed using the corresponding osABKARs (Fig. 5c). AIPs and organelle-specific AIPs are encoded on plasmids, which can be co-transfected with ABKAR. Hence, the experimental protocol is similar to that described in Subheading 3.

4 Notes

1. Use appropriate concentration of trypsin based on the adhesivity of the cell. Prolonged trypsin treatment will damage cells and may change the phenotype.

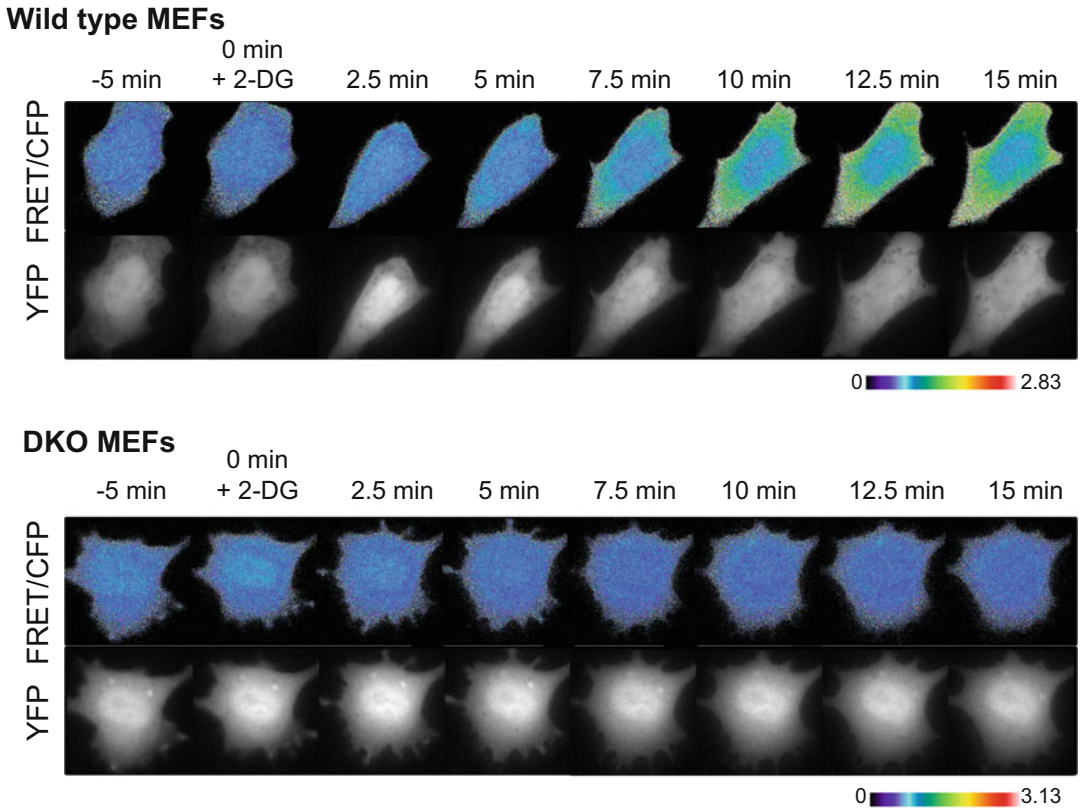

Fig. 4 Representative FRET image in wild-type MEFs and AMPK α subunit double knockout (DKO) MEFs as measured by ABKAR. Cells were treated with 10 mM 2-DG. Reproduced from [11] with permission

2. Our prior experience indicates that the use of FuGENE HD reagent with antibiotics does not cause cytotoxicity nor drop in transfection efficiency for mouse embryonic fibroblasts (MEFs), African green monkey fibroblast cells (Cos7), human cervical cancer cells (HeLa), and human embryonic kidney cells (HEK293).
3. In our protocol, 2-DG was dissolved in distilled Milli-Q water and was used at a final concentration of 10 mM.
4. If the concentration of nutrients, especially glucose, in the cell culture medium is considerably different from the imaging media, it is suggested to check whether the difference affects AMPK activity with a Western blot to detect phosphorylation level of AMPK Thr172 and AMPK substrate ACC Ser79.
5. When imaging in the absence of a stage CO_2 incubator, fluctuations in pH levels become a critical issue in FRET measurements and AMPK activity. Addition of HEPES in medium can mitigate this issue by maintaining the pH at physiological level for at least 30 min.

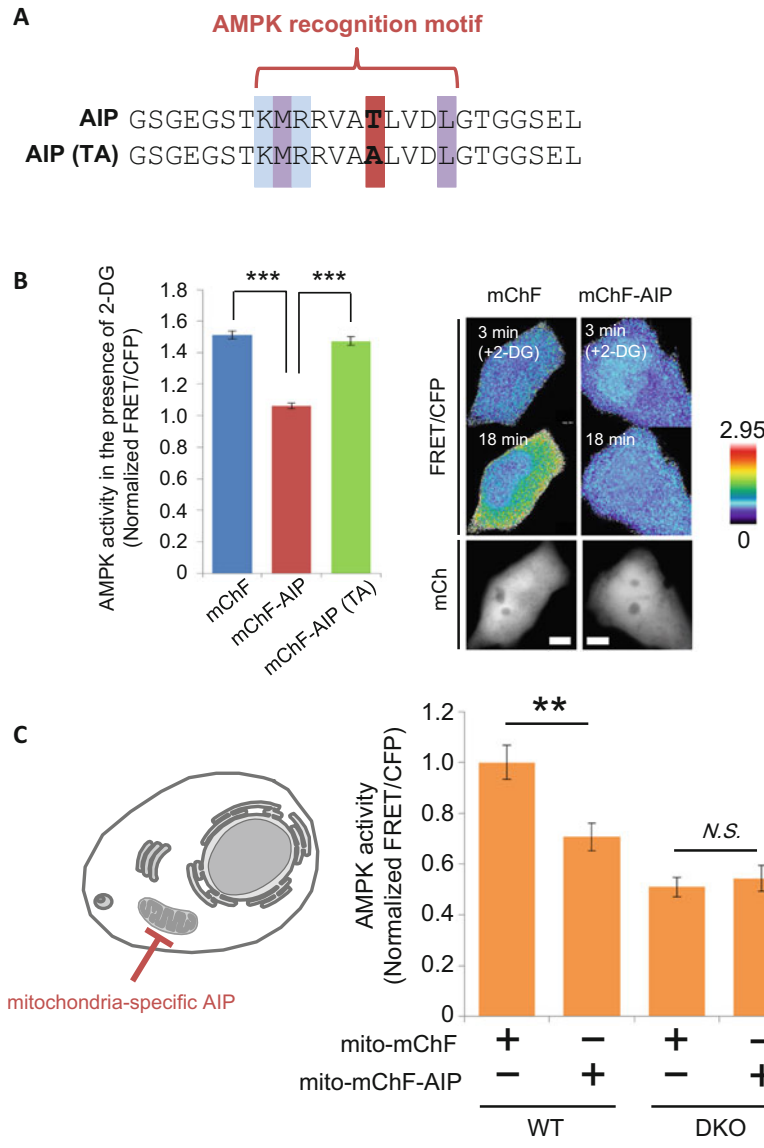

Fig. 5 Development of AIP. (**a**) The alignment of the amino acid sequences of AIP and AIP (TA) is shown. (**b**) The degree of AMPK inhibition of each AIP is shown. Cos7 cells expressing ABKAR and either mChF (control), mChF-AIP, or mChF-AIP (TA) were treated with 10 mM 2-DG for 20 min. (*Left*) The average of normalized FRET/CFP ratio from 15 to 20 min are shown as mean ± SD. (*Right*) Representative pseudocolor images of FRET/CFP ratio in cells expressing either mChF or mChF-AIP are shown. Reproduced from [11] with permission. (**c**) Inhibition of AMPK activity at mitochondria. WT MEFs and AMPK α subunit double knockout (DKO) MEFs were transiently transfected with either mito-mChF or mito-mChF-AIP, and AMPK activity was measured at the mitochondria under nutrient-surplus condition by mito-ABKAR. Quantification was performed on three independent experiments. Data are presented as mean ± SD. Reproduced from [11] with permission

6. Phenol red increases background fluorescence which interferes with the FRET signal; thus it is recommended to use phenol red-free medium for imaging.

7. Alternative image analysis can be used. FRET analysis requires image analysis software capable of performing basic arithmetic operations on images.
8. The information on OTSs for the nucleus, mitochondria, lysosome, peroxisome, ER, plasma membrane, Golgi apparatus, and secretory pathway is available in LocSigDB (http://genome.unmc.edu/LocSigDB/index.html).
9. Some general restriction enzymes are available for appending compartment-targeting sequences at either end of ABKAR. However, in cases where embedded restriction enzyme site (s) exists within the compartment-targeting sequences, infusion cloning may circumvent the problem.
10. OTSs were fused to ABKARs by designing oligonucleotides that were flanked by specific restriction enzyme sites. Cutting them with the respective restrictive enzymes provide sticky ends that can be used to ligate the OTSs to the desired location in the ABKAR containing plasmid.
11. Appropriate culture medium should be used according to ATCC protocol.
12. Prolonged incubation (>1 h) reduces transfection efficiency of FuGENE HD in MEFs. For better reproducibility, incubation time should be fixed.
13. To prepare Poly-D-lysine-coated cover slips, sterilize round glass cover slips with absolute ethanol, air-dry them and apply 100 μl of poly-D-lysine solution to each cover slip. Incubate for 2 min at room temperature and wash twice with 500 μl of sterile Milli-Q water. It is not necessary to coat the entire surface of the glass cover slips. A droplet with diameter of 5 mm is enough for the experiment. Most cell types may require this procedure unless the cell type is highly adherent to the cover slips.
14. AMPK shows disparate activation dynamics at the subcellular compartment level in response to cell confluence status [17]. Therefore, appropriate cell confluency for each experiment should be determined.
15. For better reproducibility, culture time should be fixed.
16. When analyzing metabolic signaling pathways, it is recommended to replace old medium with a fresh one to keep AMPK activity at basal level before imaging, because AMPK activity is highly sensitive to the cellular environment.
17. Imaging medium should be at room temperature unless a different temperature is required.
18. Since AMPK activity fluctuates in response to cellular environmental changes (such as temperature and medium pH),

optimization of imaging conditions is a prerequisite. To optimize imaging conditions, it is advisable to monitor AMPK activity under control condition (e.g., nutrient-rich condition).

19. In addition to optimizing imaging conditions, preparation of AMPK α1 and α2 subunit-deficient cells is important to validate the results obtained from ABKAR. It should be noted that ABKAR is not specific for AMPK; brain-specific kinases 1 and 2 (BRSK1 and BRSK2) are able to phosphorylate and change FRET signals of ABKAR [13]. Appropriate control experiments will help control for any AMPK-independent effects.
20. If the fluorescence measurements of the cell of interest are either saturated or indistinguishable from the background, it is recommended to exclude it from the analysis. To identify abnormal organelle morphology, compare cells with a control in which an appropriate organelle marker is expressed. If the cell of interest does not fall into the pool of control cells which constitutes 95% of the total population of cells when grouped by morphological similarity, the cell of interest should not be considered in the analysis.
21. It has been revealed that 2-DG treatment induces AMPK activation in the cytosol, but not in the nucleus, whereas ionomycin is able to increase AMPK activity in both compartments [10, 11]. It is good to keep in mind that different stimuli could cause different activation pattern of AMPK spatiotemporally.
22. It is advisable to monitor AMPK activity at least 5 min without adding any stimulants to make sure the imaging conditions do not affect AMPK activity as monitored by the osABKARs.
23. It should be kept in mind that AMPK activity in certain organelles is not uniform. Therefore, it is advisable to take at least three ROIs at the compartment of interest per single cell and obtain the average. The size of the ROI should be just enough to cover the compartment so that extraneous signal does not get incorporated into the measurement.
24. To calculate the corrected FRET, it is necessary to go through a number of image processing steps. To obtain the fraction of excitation cross talk "CT_{YFP}," excite cells expressing only YFP with a 504 nm laser, each time collecting the images in the YFP and FRET detection channels. It is best to use a diffusive protein to estimate cross talks to avoid FRET artifacts. Collect ten cells and measure the fluorescence signal of each cell with an image processing software.

$$\Upsilon_i = \frac{\left(\mathrm{FRET}_{\mathrm{ex427nm},i}\right) - \mathrm{background}}{\left(\mathrm{YFP}_{\mathrm{ex504nm},i}\right) - \mathrm{background}}$$

Repeat this calculation for each cell and take the average from the following equation:

$$CT_{YFP} = \sum_{1}^{10} \Upsilon_i / 10.$$

To calculate emission cross talk "CT_{CFP}," excite cells expressing only CFP with a 427 nm laser and collect images in the CFP and FRET detection channels. Again collect ten cells and measure the fluorescence.

$$C_i = \frac{\left(FRET_{ex427nm,i}\right) - \text{background}}{\left(CFP_{ex427nm,i}\right) - \text{background}}$$

Repeat this calculation for each cell and take the average from the following equation:

$$CT_{CFP} = \sum_{1}^{10} C_i / 10.$$

The corrected FRET ($FRET_C$) can be calculated by the following equation:

$$FRET_C = FRET_{raw} - CT_{YFP} * YFP - CT_{CFP} * CFP.$$

For further information, refer to [18].

25. Subcellular compartment-specific AMPK biosensors are powerful tools to detect compartmentalized AMPK signaling. However, one must be aware of the fact that OTS, itself, can influence the sensitivity of the sensor. Accordingly, the dynamic range of the osABKARs varied across subcellular compartments as a result of the modifications (Fig. 6). Therefore, it is vital that one does not directly compare AMPK activity at subcellular compartments with the FRET signals reported by the different osABKARs.
26. The current amino acid sequence of AIP was designed according to the data from a positional scanning peptide library screen (Fig. 5a) [10, 11]. However, it is essential to note that BRSK1 and BRSK2 can phosphorylate AIP as described in **Note 4**, hence, inhibiting BRSK1/2 in a competitive manner. To avoid misinterpreting the results, it is necessary to have an appropriate control experiment (e.g., AMPK-knockout cells).
27. In the case of transfection of MEFs, optimal ratio of plasmids encoding ABKAR and AIP is 1:1. But it is dependent on experimental conditions (cell lines, transfection reagents, etc.).

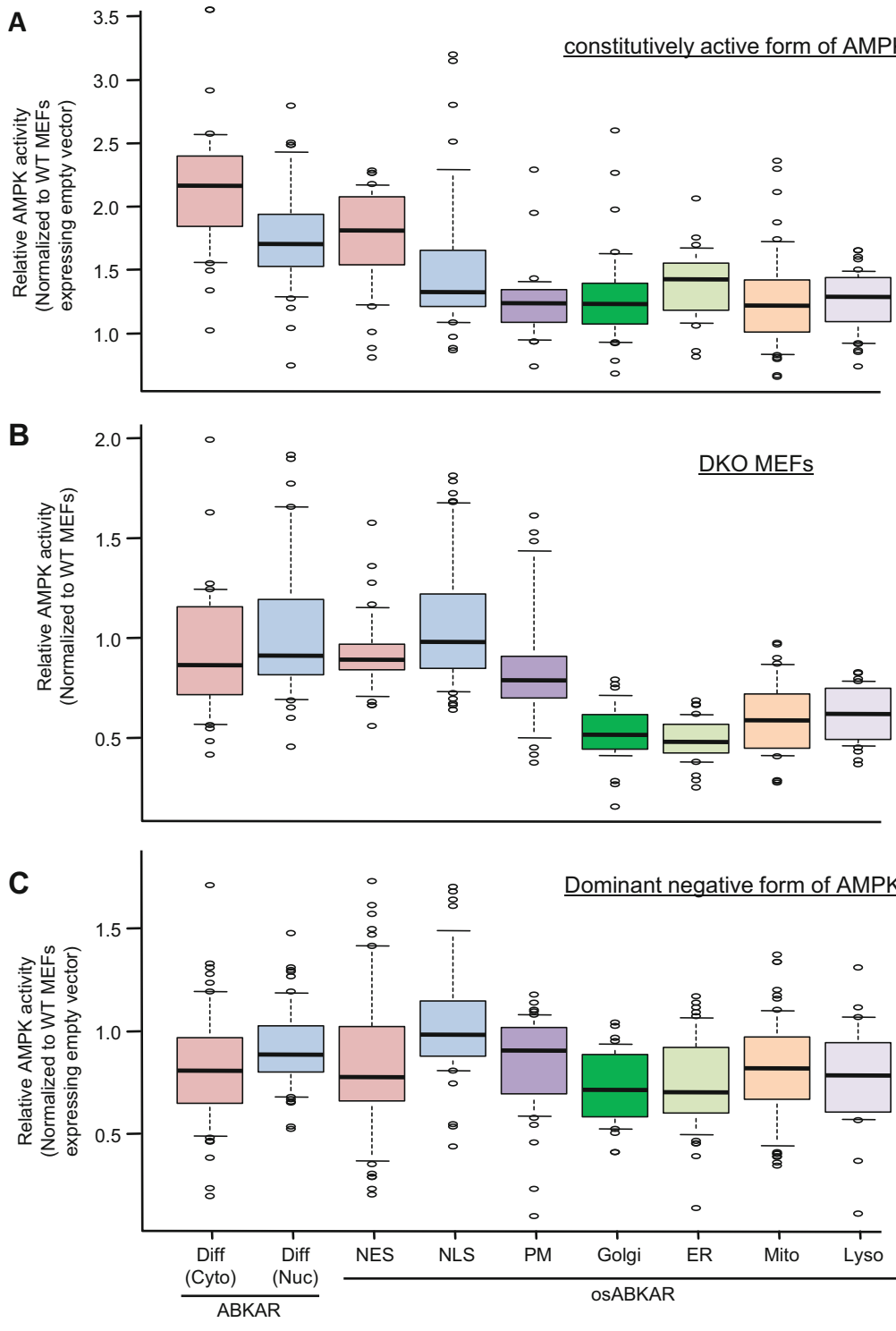

Fig. 6 Dynamic range of ABKAR and osABKARs is shown. The dynamic range of each AMPK biosensor was obtained from wild-type mouse embryonic fibroblasts (MEFs) expressing a constitutively active form of AMPK (**a**), AMPK α subunit double knockout MEFs (**b**), and wild-type MEFs expressing a dominant negative form of AMPK (**c**) under nutrient-rich condition. Reproduced from [11] with permission

Acknowledgments

We are grateful to Robert DeRose and Daniel Frigo for constructive comments. This work was supported in part by the US National Institutes of Health (NIH) grant to T.I. (DK102910).

References

1. Hardie DG, Ross FA, Hawley SA (2012) AMPK: a nutrient and energy sensor that maintains energy homeostasis. Nat Rev Mol Cell Biol 13:251–262
2. Shackelford DB, Shaw RJ (2009) The LKB1-AMPK pathway: metabolism and growth control in tumour suppression. Nat Rev Cancer 9:563–575
3. Xiao B, Sanders MJ, Underwood E et al (2011) Structure of mammalian AMPK and its regulation by ADP. Nature 472:230–233
4. Oakhill JS, Steel R, Chen Z et al (2011) AMPK is a direct adenylate charge-regulated protein kinase. Science 332:1433–1435
5. Woods A, Johnstone SR, Dickerson K et al (2003) LKB1 is the upstream kinase in the AMP-activated protein kinase cascade. Curr Biol 13:2004–2008
6. Hawley SA, Pan DA, Mustard KJ et al (2005) Calmodulin-dependent protein kinase kinase-beta is an alternative upstream kinase for AMP-activated protein kinase. Cell Metab 2:9–19
7. Woods A, Dickerson K, Heath R et al (2005) Ca2+/calmodulin-dependent protein kinase kinase-beta acts upstream of AMP-activated protein kinase in mammalian cells. Cell Metab 2:21–33
8. Schaffer BE, Levin RS, Hertz NT et al (2015) Identification of AMPK phosphorylation sites reveals a network of proteins involved in cell invasion and facilitates large-scale substrate prediction. Cell Metab 22:907–921
9. Medints I, Hildebrandt N (2013) FRET – Förster Resonance Energy Transfer: from theory to applications. Wiley Online Library. http://onlinelibrary.wiley.com/book/10.1002/9783527656028
10. Tsou P, Zheng B, Hsu C-H et al (2011) A fluorescent reporter of AMPK activity and cellular energy stress. Cell Metab 13:476–486
11. Miyamoto T, Rho E, Sample V et al (2015) Compartmentalized AMPK signaling illuminated by genetically encoded molecular sensors and actuators. Cell Rep 11:657–670
12. Miyamoto T, Rho E, Inoue T (2015) Deconvoluting AMPK dynamics. Oncotarget 6:30431–30432
13. Sample V, Ramamurthy S, Gorshkov K et al (2015) Polarized activities of AMPK and BRSK in primary hippocampal neurons. Mol Biol Cell 26:1935–1946
14. Depry C, Mehta S, Li R, Zhang J (2015) Visualization of compartmentalized kinase activity dynamics using adaptable BimKARs. Chem Biol 22:1470–1480
15. DeRose R, Miyamoto T, Inoue T (2013) Manipulating signaling at will: chemically-inducible dimerization (CID) techniques resolve problems in cell biology. Pflugers Arch 465:409–417
16. Komatsu T, Inoue T (2014) A method to rapidly induce organelle-specific molecular activities and membrane tethering. Methods Mol Biol 1174:231–245
17. Kodiha M, Rassi JG, Brown CM, Stochaj U (2007) Localization of AMP kinase is regulated by stress, cell density, and signaling through the MEK-->ERK1/2 pathway. Am J Physiol Cell Physiol 293:C1427–C1436
18. Fivaz M, Bandara S, Inoue T, Meyer T (2008) Robust neuronal symmetry breaking by Ras-triggered local positive feedback. Curr Biol 18:44–50